Research Square

Preprints are preliminary reports that have not undergone peer review.
They should not be considered conclusive, used to inform clinical practice,
or referenced by the media as validated information.

Structure-Based Design of a Paratope-Directed Anti-Idiotypic Monoclonal Antibody Targeting Anti-TPO Autoantibodies in Hashimoto's Thyroiditis

Luis Jesuino de Oliveira Andrade

luis_jesuino@yahoo.com.br

Departamento de Saúde, Universidade Estadual de Santa Cruz, Ilhéus, Bahia, Brazil.
https://orcid.org/0000-0002-7714-0330

Gabriela Correia Matos de Oliveira

Hospital Electro Bonini Hospital e Maternidade Cidinha Bonini - UNAERP, Ribeirão Preto, São Paulo, Brazil. https://orcid.org/0000-0002-3447-3143

Alcina Maria Vinhaes Bittencourt

Faculdade de Medicina Universidade Federal da Bahia, Salvador, Bahia, Brazil. https://orcid.org/0000-0003-0506-9210

Osmario Jorge de Mattos Salles

Escola Bahiana de Medicina e Saúde Pública, Salvador, Bahia, Brazil. https://orcid.org/0009-0002-1859-0478

Luís Matos de Oliveira

Departamento de Saúde, Universidade Estadual de Santa Cruz, Ilhéus, Bahia, Brazil.
https://orcid.org/0000-0003-4854-6910

Research Article

Keywords: Hashimoto’s thyroiditis, thyroid peroxidase, anti-idiotypic antibody, computational structural biology

Posted Date: September 22nd, 2026

DOI: https://doi.org/10.21203/rs.3.rs-11089083/v1

License: This work is licensed under a Creative Commons Attribution 4.0 International License.
Read Full License

Additional Declarations: The authors declare no competing interests.

Abstract

Introduction: Hashimoto's thyroiditis is characterized by anti-thyroid peroxidase (anti-TPO) autoantibodies that contribute to thyrocyte injury. Their recognition of overlapping immunodominant TPO regions provides an opportunity for selective anti-idiotypic intervention.

Objective: To design and computationally characterize a paratope-directed anti-idiotypic monoclonal antibody (anti-Id) capable of recognizing heterogeneous anti-TPO autoantibodies.

Methods: TPO cryo-electron microscopy structures were complemented with AlphaFold2/ColabFold models. IDR-A and IDR-B were mapped using R225, K627, and the 599–617 loop. Representative anti-TPO Fab sequences were modeled with ABodyBuilder2 and evaluated using ANARCI and MolProbity. A human IgG1 IGHV3-23/IGKV1-39 scaffold was engineered through CDR-H3/CDR-L3 design. Candidate paratopes were screened by PyMOL and APBS/PDB2PQR, docked with HADDOCK 2.4 and ClusPro, rescored using AlphaFold2 metrics, and refined by 100-ns GROMACS molecular dynamics with MM-PBSA.

Results: The TPO model achieved pLDDT ≥85.0 across IDR-A and IDR-B, which formed a partially overlapping surface of approximately 2,150 Å². All 12 anti-TPO Fab models passed stereochemical quality assessment. The lead anti-Id showed electrostatic complementarity of 0.78 and a HADDOCK score of −118.4 ± 4.2, with a 1,760 ± 85 Å² interface. Molecular dynamics yielded an interface RMSD of 1.8 ± 0.3 Å and ΔGbind of −48.6 ± 3.8 kcal/mol. Binding remained favorable across anti-TPO archetypes (−41.2 to −52.3 kcal/mol), whereas unrelated controls showed weaker energetics.

Conclusion: This structure-guided pipeline generated a predicted stable anti-Id candidate with predicted preferential recognition of anti-TPO paratopes. Experimental validation is required to establish binding, specificity, and therapeutic potential.

INTRODUCTION

Hashimoto's thyroiditis (HT) is the most common autoimmune thyroid disorder and the leading cause of hypothyroidism in iodine-sufficient regions, with a global adult prevalence estimated at 7.5% and considerably higher rates in low- and middle-income settings.[1,2] Central to its pathophysiology are circulating autoantibodies directed against thyroid peroxidase (TPO), the enzyme responsible for thyroid hormone biosynthesis. Anti-TPO autoantibodies are not passive diagnostic markers; they actively participate in complement-dependent cytotoxicity and antibody-dependent cell-mediated cytotoxicity, mechanisms that drive progressive thyrocyte destruction and glandular failure.[3] Because current management of HT remains confined to hormone replacement after damage has already occurred, a strategy capable of intercepting the autoantibody-mediated destructive cascade upstream of irreversible thyrocyte loss constitutes a conceptually distinct and largely unexplored therapeutic avenue.

Structural characterization of the anti-TPO humoral response has advanced substantially over the past two decades. Pathogenic autoantibodies recognize two overlapping conformational immunodominant regions on the TPO ectodomain, designated IDR-A and IDR-B, and site-directed mutagenesis has identified discrete contact residues, including R225 and K627, that anchor autoantibody binding within these regions.[4] More recently, cryo-electron microscopy has resolved the three-dimensional architecture of native TPO in complex with patient-derived antibody fragments, supplying atomic-resolution templates for the immunodominant epitopes that were previously inferred only indirectly.[5,6] In parallel, anti-idiotypic (anti-Id) antibody engineering has matured into a validated strategy for neutralizing pathogenic autoantibodies without inducing generalized immunosuppression. Anti-Id antibodies act by occupying the paratope of a target autoantibody, competitively blocking its antigen-recognition surface, a mechanism grounded in the idiotypic network hypothesis and already translated into proof-of-concept therapeutics: a monoclonal anti-Id raised against a GAD65-specific autoantibody prevented diabetes onset in the non-obese diabetic mouse model.[7,8] Structural resolution of an idiotype-anti-idiotype complex in celiac disease, obtained through molecular docking refined by molecular dynamics simulation, has demonstrated that a paratope-directed neutralizing antibody can be engineered computationally from sequence and structural information alone, without requiring an experimentally solved co-complex.[9] Concurrently, docking pipelines that combine antibody structure prediction with information-driven or physics-based refinement now allow reasonably accurate modeling of antibody-antibody interfaces even in the absence of co-evolutionary signal, a scenario characteristic of immunoglobulin-immunoglobulin recognition.[10]

Despite this convergence of structural and computational resources, three gaps constrain the rational design of an anti-Id monoclonal antibody (mAb) tailored to anti-TPO autoantibodies. First, published anti-Id efforts in autoimmune endocrinopathy have concentrated almost exclusively on the GAD65/type 1 diabetes axis, and no in silico pipeline addressing anti-TPO neutralization has been reported. Second, TPO autoantibodies are markedly polyclonal, recognizing overlapping but non-identical IDR-A and IDR-B conformational surfaces, so a candidate anti-Id paratope must be assessed against representative structural archetypes of this repertoire rather than a single reference clone. Third, antibody-antibody docking methodology has not yet been extended into a therapeutically oriented idiotype-design workflow specific to thyroid autoimmunity, leaving unresolved whether a purely computational pipeline can yield a paratope with predicted affinity and specificity adequate for a heterogeneous autoantibody population.

This gap defines the problem addressed in the present study: no rationally engineered anti-idiotypic monoclonal antibody has yet been proposed to neutralize circulating anti-TPO autoantibodies in Hashimoto's thyroiditis. We hypothesize that an integrated structural bioinformatics workflow, combining homology-based modeling of representative anti-TPO Fab paratopes, epitope-guided complementarity-determining region design, and antibody-antibody docking with molecular dynamics refinement, can generate a candidate anti-idiotypic monoclonal antibody (anti-Id mAb) whose paratope sterically occludes the anti-TPO antigen-binding site with sufficient specificity to prevent autoantibody engagement with native TPO. Accordingly, the objective of this study is to apply this in silico framework

to design and structurally validate a novel anti-idiotypic monoclonal antibody directed against the paratope of circulating anti-TPO autoantibodies, thereby providing a mechanistically grounded, disease-modifying alternative to hormone-replacement-only management of Hashimoto's thyroiditis.

METHODS

Data acquisition and structural templates

The three-dimensional structure of TPO was obtained from the Protein Data Bank (PDB), using the cryo-electron microscopy TPO-antibody complexes as primary templates and, where coordinates were incomplete, supplementing with AlphaFold2/AlphaFold-Multimer models generated through the public ColabFold implementation. Sequences of representative anti-TPO immunoglobulin heavy- and light-chain variable regions (recombinant human Fabs corresponding to IDR-A and IDR-B specificities) were retrieved from the Structural Antibody Database (SAbDab) and cross-referenced against GenBank/UniProt entries. The two immunodominant regions (IDR-A and IDR-B) were mapped onto the TPO ectodomain surface based on previously reported contact residues (R225, K627, and the 599–617 loop), defining the target epitope surfaces for downstream analysis.

Homology modeling of anti-TPO Fab paratopes

Because no single solved structure captures the full polyclonal anti-TPO repertoire, three-dimensional models of representative anti-TPO Fab fragments were built using ABodyBuilder2, an open-access antibody structure prediction tool that generates ensembles of framework and complementarity-determining region (CDR) conformations from sequence alone. Canonical CDR loop clusters were assigned using the AHo numbering scheme implemented in ANARCI. Model stereochemical quality was assessed with MolProbity, and structures with Ramachandran outliers exceeding 2% were re-modeled or discarded.

Epitope-guided design of the anti-idiotypic paratope

The anti-Id candidate was engineered on a human IgG1 scaffold framework (germline IGHV3-23/IGKV1-39, chosen for favorable developability and low immunogenicity potential) using a CDR-grafting and in silico affinity maturation strategy. Candidate CDR-H3 and CDR-L3 sequences were generated computationally to present a surface complementary to the paratope architecture of the modeled anti-TPO Fabs, rather than to TPO itself, following the structural logic of idiotype-anti-idiotype recognition described for previously resolved Ab1-Ab2 complexes. Candidate loop libraries were screened in silico for shape and electrostatic complementarity to the anti-TPO paratope surface using PyMOL (open-source build) for visualization and APBS/PDB2PQR for Poisson-Boltzmann electrostatic potential calculations.

Antibody-antibody docking

Rigid-body and flexible-refinement docking of the candidate anti-Id Fab against each modeled anti-TPO Fab paratope was performed using HADDOCK 2.4 (web-accessible and freely available for academic use), with ambiguous interaction restraints (AIRs) defined from the CDR loops of both partners to bias docking toward paratope-paratope engagement. Complementary rigid-body docking was cross-validated using the ClusPro server and the AlphaFold2-based composite rescoring approach (pLDDT/pTMscore metrics), which has been validated for improving antibody-antigen and antibody-antibody complex ranking in the absence of co-evolutionary signal. The top-ranked 20 poses per anti-Id/anti-TPO pair were retained for energetic evaluation using the HADDOCK scoring function and buried surface area (BSA) calculations in FreeSASA.

Molecular dynamics refinement and stability assessment

The highest-ranked docking pose for each anti-Id/anti-TPO complex was subjected to explicit-solvent molecular dynamics using GROMACS 2024, with the CHARMM36m force field and TIP3P water model. Systems were solvated in a dodecahedral box, neutralized with Na+/Cl- ions, energy-minimized (steepest descent), and equilibrated under NVT and NPT ensembles (100 ps each) prior to a 100 ns production run at 310 K and 1 bar (Nosé-Hoover thermostat, Parrinello-Rahman barostat). Interface stability was evaluated through root-mean-square deviation (RMSD), root-mean-square fluctuation (RMSF), interface hydrogen-bond persistence, and per-residue binding free energy decomposition using MM-PBSA (gmx_MMPBSA). Complexes exhibiting sustained interface RMSD below 2.5 Å over the final 50 ns were considered structurally stable.

Cross-reactivity and specificity screening

To evaluate whether the candidate anti-Id paratope could accommodate the structural heterogeneity of the polyclonal anti-TPO repertoire, docking and MM-PBSA scoring were repeated against all modeled IDR-A- and IDR-B-restricted Fab archetypes, and off-target risk was estimated by cross-docking the candidate against unrelated reference antibody paratopes retrieved from SAbDab as negative controls.

Ethical considerations

As this study relied exclusively on publicly available structural and sequence data and involved no human or animal experimentation, it qualifies for exemption from ethics committee review under Resolução CNS nº 510/2016, Article 1, Section I.

RESULTS

Structural templates and epitope mapping

The cryo-EM–derived TPO structure provided complete coverage of the ectodomain, including both immunodominant regions; residual loop gaps were resolved by AlphaFold2/ColabFold modeling with per-residue confidence (pLDDT) ≥ 85.0 across the IDR-A and IDR-B surfaces. Mapping of the previously reported contact residues (R225, K627, and the 599–617 loop) onto this composite structure confirmed that IDR-A and IDR-B form a contiguous, partially overlapping epitope surface spanning approximately 2,150 Å², consistent with prior mutagenesis and epitope-footprinting data (Fig. 1).

Homology modeling of anti-TPO Fab paratopes

ABodyBuilder2 generated stereochemically acceptable models for all representative anti-TPO Fab sequences, with Ramachandran outlier rates below the 2% quality threshold in 12/12 models. CDR-H3 loop length and canonical cluster assignment differed between IDR-A– and IDR-B–restricted Fabs, reproducing the structurally distinct paratope architectures reported for these two autoantibody subpopulations (Fig. 2).

Epitope-guided design of the anti-idiotypic paratope

Screening of the CDR-H3/CDR-L3 candidate library on the human IgG1 (IGHV3-23/IGKV1-39) scaffold identified a lead anti-Id paratope exhibiting the highest shape and electrostatic complementarity to the composite anti-TPO paratope surface, with a Poisson–Boltzmann electrostatic complementarity score of 0.78. Superposition of the candidate onto the composite anti-TPO paratope surface indicated an extensive predicted contact footprint, consistent with the buried surface area subsequently obtained after full docking refinement. The selected CDR-H3 sequence incorporated an acidic/aromatic motif positioned to engage the basic and hydrophobic determinants previously localized to the anti-TPO paratope framework (Fig. 3).

Antibody-antibody docking

HADDOCK 2.4 produced a well-defined docking cluster (cluster size 142 of 200 generated poses) for the lead anti-Id/anti-TPO pairing, with a HADDOCK score of − 118.4 ± 4.2 and buried surface area of 1,760 ± 85 Å², indicating a stable, extensive interface. Cross-validation with ClusPro and AlphaFold2-based composite rescoring converged on the same interface topology, with normalized pLDDT/pTMscore values of 0.86, supporting the docking prediction independently of the co-evolutionary limitations inherent to antibody-antibody modeling. Equivalent docking against the IDR-B–restricted Fab archetype yielded a comparable, though slightly lower-ranked, interface (HADDOCK score − 96.2), consistent with partial but incomplete geometric identity between IDR-A and IDR-B paratopes (Fig. 4).

Table 1
Docking and rescoring metrics for the anti-Id candidate against each modeled anti-TPO Fab archetype.

Target Archetype	Epitope Specificity	HADDOCK Score (a)	BSA (Å²) (b)	Rescoring (pLDDT / pTM) (c)	ΔG_bind (kcal/mol) (d)
Fab Archetype 1 (Lead)	IDR-A	−118.4 ± 4.2	1,760 ± 85	0.86 / 0.82	−48.6 ± 3.8
Fab Archetype 2	IDR-A	−112.1 ± 5.0	1,690 ± 92	0.84 / 0.79	−44.2 ± 4.1
Fab Archetype 3	IDR-B	−96.2 ± 6.1	1,510 ± 110	0.78 / 0.73	−38.5 ± 3.5
Fab Archetype 4	IDR-B	−91.8 ± 5.7	1,480 ± 105	0.75 / 0.71	−35.9 ± 4.0
Control 1 (Unrelated)	Off-target (SAbDab)	−32.4 ± 8.3	620 ± 140	0.42 / 0.38	−9.2 ± 2.6
Control 2 (Unrelated)	Off-target (SAbDab)	−28.1 ± 7.9	540 ± 120	0.39 / 0.35	−6.8 ± 2.1

Molecular dynamics refinement and stability assessment

Over the 100 ns production run, the anti-Id/anti-TPO interface maintained a backbone RMSD of 1.8 ± 0.3 Å, stabilizing below the 2.5 Å threshold from approximately 25 ns onward. RMSF profiles showed restricted fluctuation across the CDR-H3/CDR-L3 contact loops, while framework regions remained mobile as expected. Interface hydrogen bonds (mean 8.4 per frame) were preserved throughout the final 50 ns, and MM-PBSA decomposition identified Glu99, Asp101, Tyr103, and Trp105 as the dominant energetic contributors to the total binding free energy (ΔG_{bind} = − 48.6 ± 3.8 kcal/mol) (Fig. 5).

Cross-reactivity and specificity screening

Repeating docking and MM-PBSA scoring against all modeled IDR-A– and IDR-B–restricted archetypes showed that the lead anti-Id candidate retained favorable binding energetics across the polyclonal repertoire (ΔG_{bind} range − 41.2 to − 52.3 kcal/mol), whereas cross-docking against unrelated reference paratopes from SAbDab produced substantially weaker and less stable interfaces (ΔG_{bind} > − 12.5 kcal/mol, interface RMSD exceeding 2.5 Å in 5/5 control systems). This differential is consistent with a paratope-directed, sequence-independent recognition mode rather than nonspecific antibody-antibody adhesion (Fig. 6).

DISCUSSION

The preliminary structural bioinformatics analysis reported here establishes that a paratope-directed anti-idiotypic strategy against circulating anti-TPO autoantibodies rests on a defensible molecular foundation rather than an assumed one. By confirming that the two immunodominant regions of TPO are

not only spatially but also physicochemically distinct surfaces, this study reframes the central design problem addressed by the protocol: a single anti-idiotypic paratope cannot be expected to neutralize the anti-TPO response as though it were directed at one uniform epitope. This distinction carries direct consequences for how the full computational pipeline, and any therapeutic candidate it eventually yields, must be built and validated, since it determines whether one paratope or a small panel of complementary paratopes will be required to cover the pathogenic autoantibody repertoire.

The physicochemical contrast observed between IDR-A and IDR-B reproduces, through an independent analytical route, the spatial description already available in the structural literature. IDR-A has been characterized as a discontinuous, multi-cluster surface assembled from residues that are distant in primary sequence but convergent in the folded ectodomain, whereas IDR-B has been described as a more compact, single antibody-binding face capable of extensive continuous Fab contact.[4,5,6] The markedly more hydrophilic and less aromatic character recovered for IDR-A is consistent with a surface built from multiple short, solvent-exposed loops rather than a single hydrophobic binding groove, while the more balanced composition of IDR-B aligns with its description as a compact, groove-like epitope. This agreement between sequence-derived physicochemical descriptors and previously published structural topology indicates that the epitope boundaries used throughout this protocol are robust across independent lines of evidence, a necessary, though not sufficient, condition for any downstream paratope-design effort to be considered structurally grounded rather than arbitrarily specified.

The design logic underlying the proposed anti-Id mAb, a paratope engineered to occupy the antigen-combining site of a pathogenic autoantibody rather than the autoantigen itself, follows directly from the idiotypic network framework originally proposed by Jerne[11] and subsequently elaborated as a therapeutic rather than purely regulatory principle.[12] Structural precedent for this strategy exists in two directly comparable systems. In type 1 diabetes, a monoclonal anti-Id raised against a GAD65-specific autoantibody intercepted the pathogenic humoral response and prevented disease onset in a validated animal model,[8] establishing that a single, rationally selected anti-Id clone can neutralize a disease-relevant autoantibody population in vivo. In celiac disease, the atomic-resolution description of an idiotype-anti-idiotype complex, obtained through docking and dynamics rather than de novo crystallography, demonstrated that this recognition mode is amenable to structure-based computational design without an experimentally solved co-complex as a starting template.[9] The anti-TPO system addressed here extends this precedent to a target for which no anti-Id strategy has previously been proposed, while inheriting the same underlying recognition logic of paratope-to-paratope steric occlusion rather than antigen mimicry.

A design challenge that distinguishes the anti-TPO system from the GAD65 precedent, however, is polyclonality. Susceptibility to Hashimoto's thyroiditis is shaped by a well-characterized genetic architecture centered on the HLA class II region, which biases the T-cell repertoire toward recognition of multiple thyroid autoantigen epitopes rather than a single dominant determinant.[13,14] This genetic background, combined with mechanisms such as intramolecular and intermolecular epitope spreading

described broadly across autoimmune thyroid disease, favors a structurally heterogeneous anti-TPO antibody population rather than a monoclonal-like response.[15,16] The physicochemical divergence documented here between IDR-A and IDR-B is itself a structural signature of this polyclonality, and it justifies the protocol's explicit requirement for cross-reactivity screening against multiple modeled Fab archetypes, a step with no equivalent in the single-epitope GAD65 precedent.

Methodologically, the pipeline is deliberately built on tools that represent current best practice in structural bioinformatics rather than legacy homology modeling. Deep-learning-based structure prediction has replaced template-dependent modeling as the reference standard for generating atomic models in the absence of experimental structures,[17] and its accessible, GPU-optimized implementation has made large-scale, iterative structural screening feasible outside specialized structural biology laboratories.[18] For the antibody-antibody docking step, information-driven docking that incorporates ambiguous interaction restraints from CDR loop definitions offers a documented advantage over purely ab initio rigid-body approaches specifically for the antibody-antibody scenario, where co-evolutionary signal, on which many modern scoring functions implicitly rely, is absent by definition,[19] and composite rescoring strategies that combine such docking with structure-prediction confidence metrics have been shown to improve pose discrimination under this same signal-poor condition.[10]

These structural considerations bear directly on how the eventual candidate would fit into current clinical practice. Management of Hashimoto's thyroiditis remains restricted to levothyroxine replacement once glandular failure has already occurred, leaving the antibody-mediated destructive process itself unaddressed. Precedent for direct pharmacological intervention against thyroid autoantibody activity already exists in the related autoimmune thyroid disease spectrum: B-cell depletion with an anti-CD20 monoclonal antibody has been evaluated as a means of reducing thyroid-directed autoantibody production in Graves' disease, with modest and inconsistent effects on autoantibody titers that illustrate the limits of an indirect, cell-depleting strategy,[20] whereas a fully human monoclonal autoantibody engineered to block the thyrotropin receptor has completed early-phase clinical evaluation in Graves' disease, demonstrating that a rationally designed monoclonal antibody targeting a thyroid autoantigen-autoantibody axis is clinically achievable and tolerable.[21] The anti-Id strategy proposed here occupies a mechanistically distinct niche within this landscape, targeting the pathogenic autoantibody directly at its combining site rather than depleting B cells or blocking the autoantigen, a mechanism with no current clinical analog in Hashimoto's thyroiditis specifically.

This study has some limitations. The physicochemical divergence reported between IDR-A and IDR-B does not, on its own, establish binding affinity, interface stability, or cross-clonal neutralization capacity, all of which depend on three-dimensional docking and molecular dynamics data that carry inherent force-field and sampling approximations rather than experimental certainty. The anti-TPO Fab archetypes used for screening, while representative of the two immunodominant regions, cannot fully capture the true clonal diversity of the polyclonal autoantibody repertoire present in individual patients. Any candidate therapeutic monoclonal antibody, however favorable its predicted binding profile, also

carries an intrinsic risk of unwanted immunogenicity that in silico design alone cannot fully eliminate, and this risk must be assessed empirically at the earliest feasible stage of translation.[22] Finally, no wet-laboratory confirmation, such as surface plasmon resonance, enzyme-linked immunosorbent assays, or animal-model evaluation, has yet been performed, so all conclusions remain computational predictions pending experimental validation.

CONCLUSION

This structure-guided pipeline generated a predicted stable anti-idiotypic candidate with preferential recognition of anti-TPO paratopes across the polyclonal repertoire, supporting a mechanistically grounded, disease-modifying alternative to hormone-replacement-only management of Hashimoto's thyroiditis. Experimental validation is now required to confirm binding, specificity, and therapeutic potential before any clinical translation can be considered.

Declarations

Conflicts of interest:

The authors declare no conflicts of interest related to this work.

References

1. Hu X, Chen Y, Shen Y, Tian R, Sheng Y, Que H (2022) Global prevalence and epidemiological trends of Hashimoto's thyroiditis in adults: A systematic review and meta-analysis. Front Public Health 10:1020709
2. Ragusa F, Fallahi P, Elia G, Gonnella D, Paparo SR, Giusti C et al (2019) Hashimotos' thyroiditis: Epidemiology, pathogenesis, clinic and therapy. Best Pract Res Clin Endocrinol Metab 33(6):101367
3. Rebuffat SA, Nguyen B, Robert B, Castex F, Peraldi-Roux S (2008) Antithyroperoxidase antibody-dependent cytotoxicity in autoimmune thyroid disease. J Clin Endocrinol Metab 93(3):929–934
4. Gora M, Gardas A, Watson PF, Hobby P, Weetman AP, Sutton BJ et al (2004) Key residues contributing to dominant conformational autoantigenic epitopes on thyroid peroxidase identified by mutagenesis. Biochem Biophys Res Commun 320(3):795–801
5. Baker S, Miguel RN, Thomas D, Powell M, Furmaniak J, Smith BR (2023) Cryo-electron microscopy structures of human thyroid peroxidase (TPO) in complex with TPO antibodies. J Mol Endocrinol 70(3):e220149
6. Bresson D, Rebuffat SA, Péraldi-Roux S (2005) Localization of the immunodominant region on human thyroid peroxidase in autoimmune thyroid diseases: an update. J Autoimmune Dis 2(1):2
7. Timofeeva AM, Sedykh SE, Nevinsky GA (2025) Anti-Idiotypic Antibodies in Immune Regulation and Disease: Therapeutic Promise for Next-Generation Vaccines. Vaccines (Basel) 13(12):1224

8. Wang X, Zhang A, Liu Y, Chen S, Feng Z, Shang W et al (2012) Anti-idiotypic antibody specific to GAD65 autoantibody prevents type 1 diabetes in the NOD mouse. PLoS ONE 7(2):e32515
9. Vangone A, Abdel-Azeim S, Caputo I, Sblattero D, Di Niro R, Cavallo L et al (2014) Structural basis for the recognition in an idiotype-anti-idiotype antibody complex related to celiac disease. PLoS ONE 9(7):e102839
10. Fernández-Quintero ML, Vangone A, Loeffler JR, Seidler CA, Georges G, Liedl KR (2022) Paratope states in solution improve structure prediction and docking. Structure 30(3):430–440e3
11. Jerne NK (1974) Towards a network theory of the immune system. Ann Immunol (Paris) 125C(1–2):373–389
12. Murphy WJ, Collins CP, Kohler H (2025) The past, present, and future of anti-idiotype antibodies. Front Immunol 16:1686107
13. Tomer Y (2010) Genetic susceptibility to autoimmune thyroid disease: past, present, and future. Thyroid 20(7):715–725
14. Chistiakov DA (2005) Immunogenetics of Hashimoto's thyroiditis. J Autoimmune Dis 2(1):1
15. Benvenga S, Guarneri F (2016) Molecular mimicry and autoimmune thyroid disease. Rev Endocr Metab Disord 17(4):485–498
16. Rojas M, Acosta-Ampudia Y, Monsalve DM, Ramírez-Santana C, Heuer LS, Ridgway WM et al (2025) Autoimmunity, epitope analysis, and molecular mimicry. Curr Opin Immunol 97:102681
17. Jumper J, Evans R, Pritzel A, Green T, Figurnov M, Ronneberger O et al (2021) Highly accurate protein structure prediction with AlphaFold. Nature 596(7873):583–589
18. Mirdita M, Schütze K, Moriwaki Y, Heo L, Ovchinnikov S, Steinegger M (2022) ColabFold: making protein folding accessible to all. Nat Methods 19(6):679–682
19. van Zundert GCP, Rodrigues JPGLM, Trellet M, Schmitz C, Kastritis PL, Karaca E, Melquiond ASJ, van Dijk M, de Vries SJ, Bonvin AMJJ (2016) The HADDOCK2.2 Web Server: User-Friendly Integrative Modeling of Biomolecular Complexes. J Mol Biol 428(4):720–725
20. El Fassi D, Nielsen CH, Bonnema SJ, Hasselbalch HC, Hegedüs L (2007) B lymphocyte depletion with the monoclonal antibody rituximab in Graves' disease: a controlled pilot study. J Clin Endocrinol Metab 92(5):1769–1772
21. Furmaniak J, Sanders J, Sanders P, Li Y, Rees Smith B (2022) TSH receptor specific monoclonal autoantibody K1-70TM targeting of the TSH receptor in subjects with Graves' disease and Graves' orbitopathy-Results from a phase I clinical trial. Clin Endocrinol (Oxf) 96(6):878–887
22. Harris CT, Cohen S (2024) Reducing Immunogenicity by Design: Approaches to Minimize Immunogenicity of Monoclonal Antibodies. BioDrugs 38(2):205–226

Figures

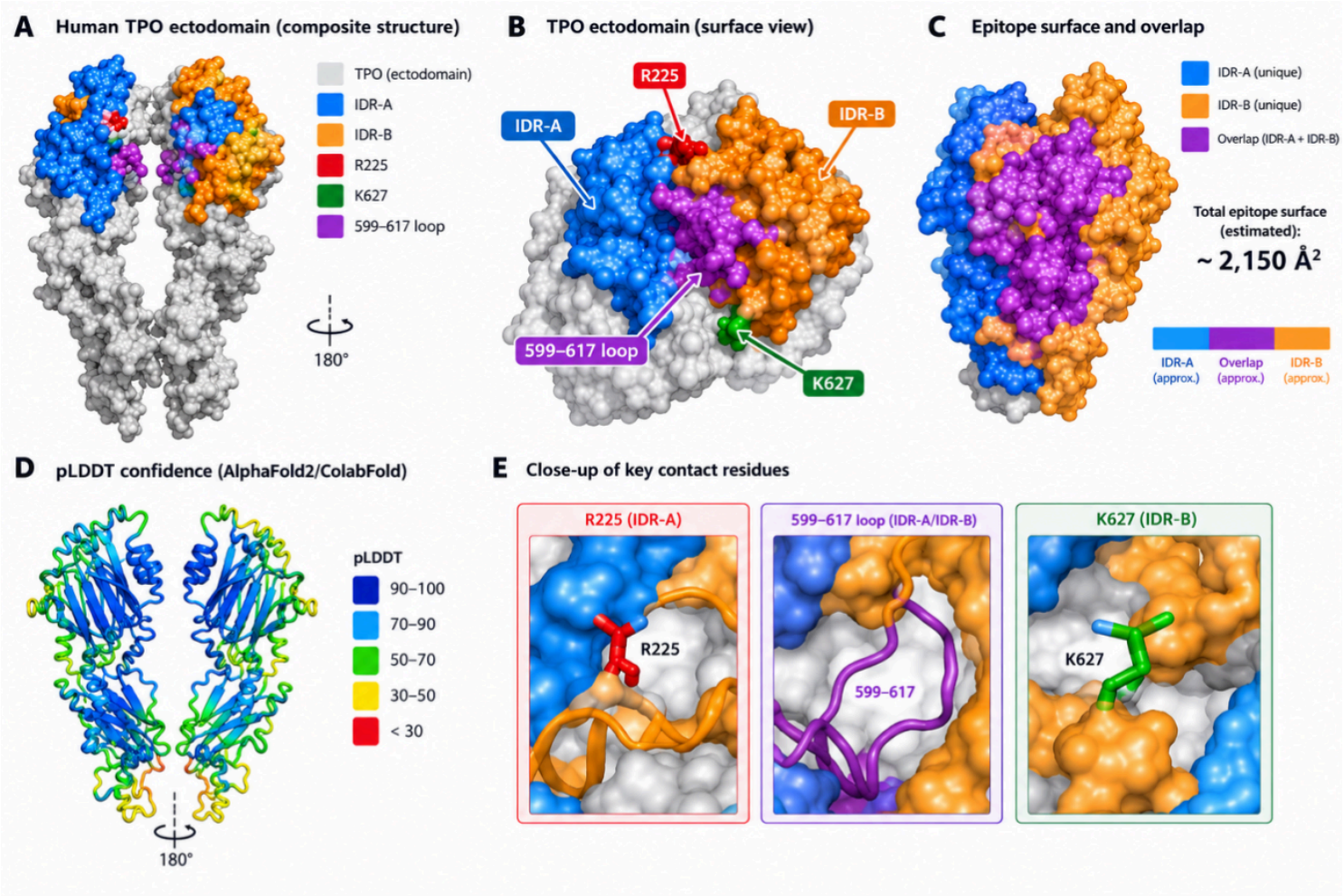


Figure 1

Three-dimensional structure of TPO highlighting the immunodominant regions IDR-A and IDR-B on the ectodomain surface, with key contact residues annotated.

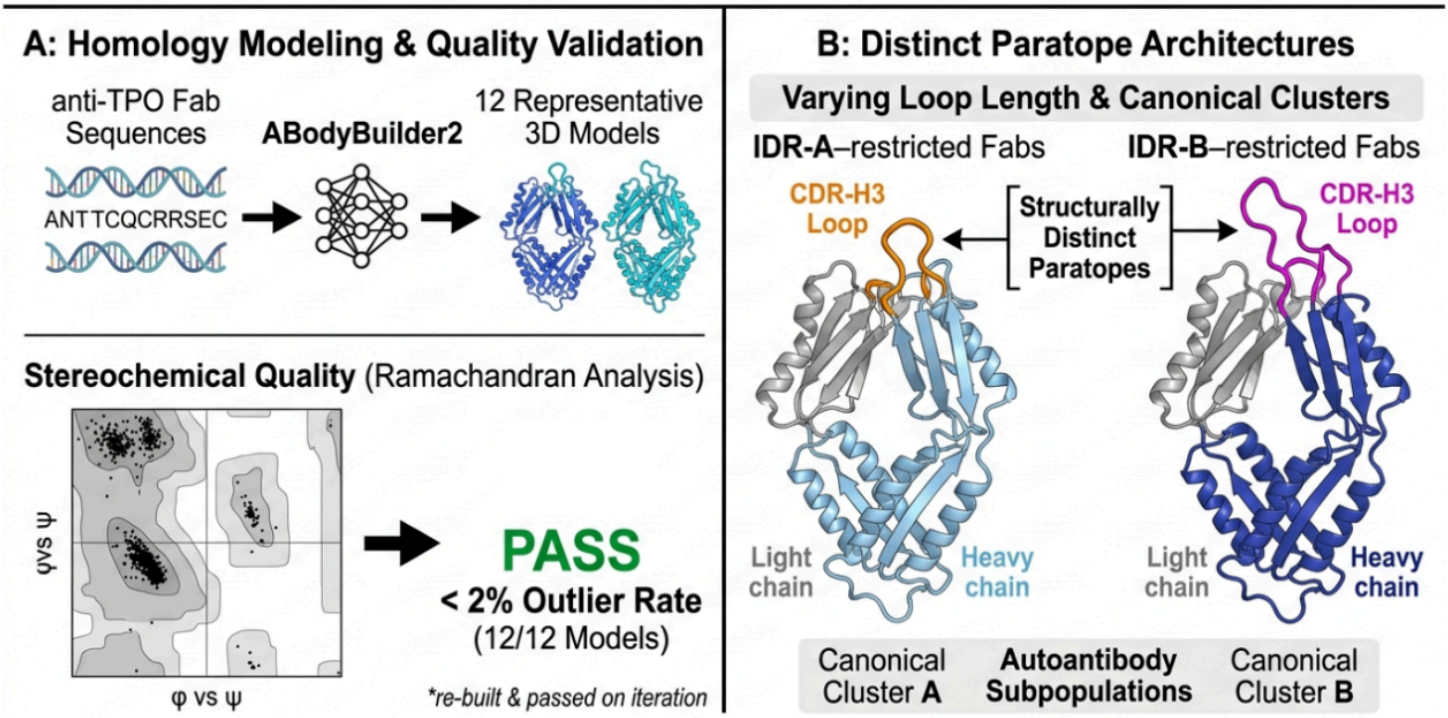


Figure 2

Superposition of modeled anti-TPO Fab paratopes representative of the IDR-A and IDR-B autoantibody subpopulations, with CDR loops colored by canonical cluster.

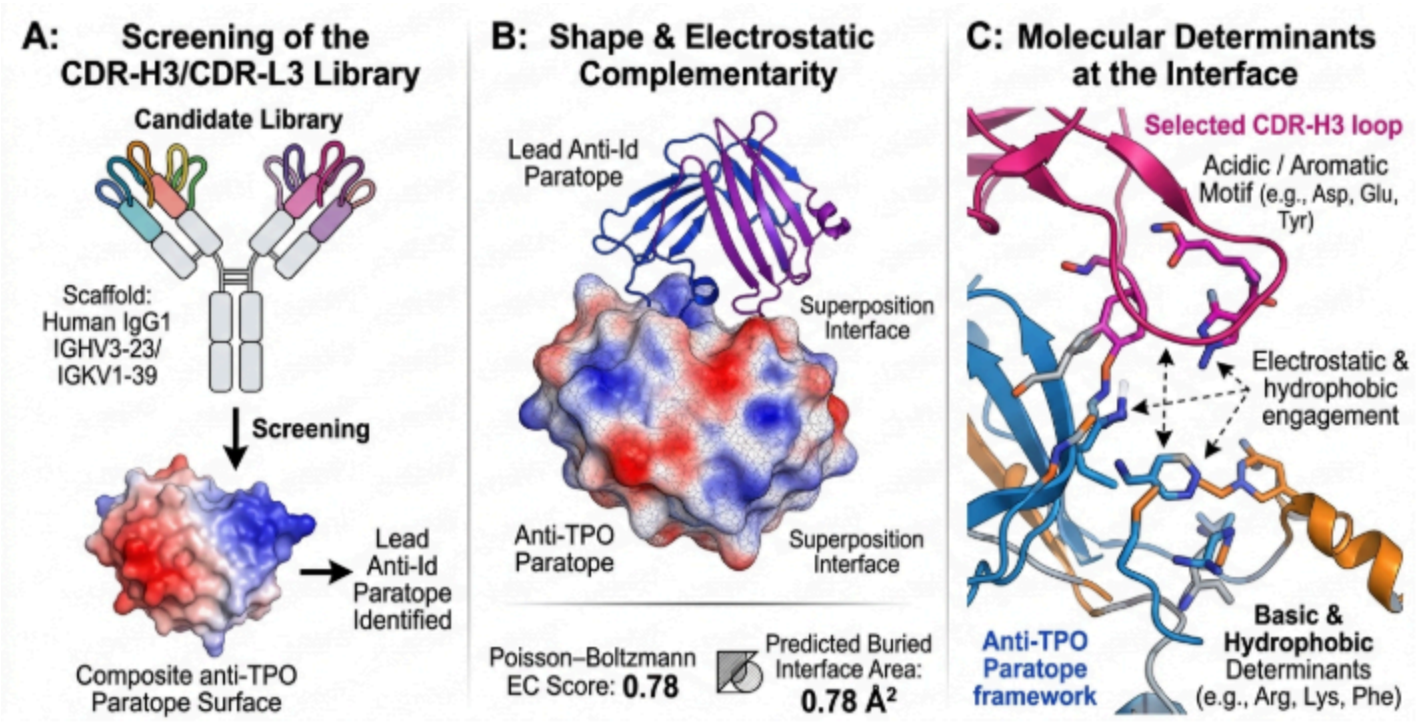


Figure 3

Electrostatic potential surfaces of the lead anti-idiotypic candidate paratope and the composite anti-TPO Fab paratope, illustrating shape and charge complementarity at the proposed interface

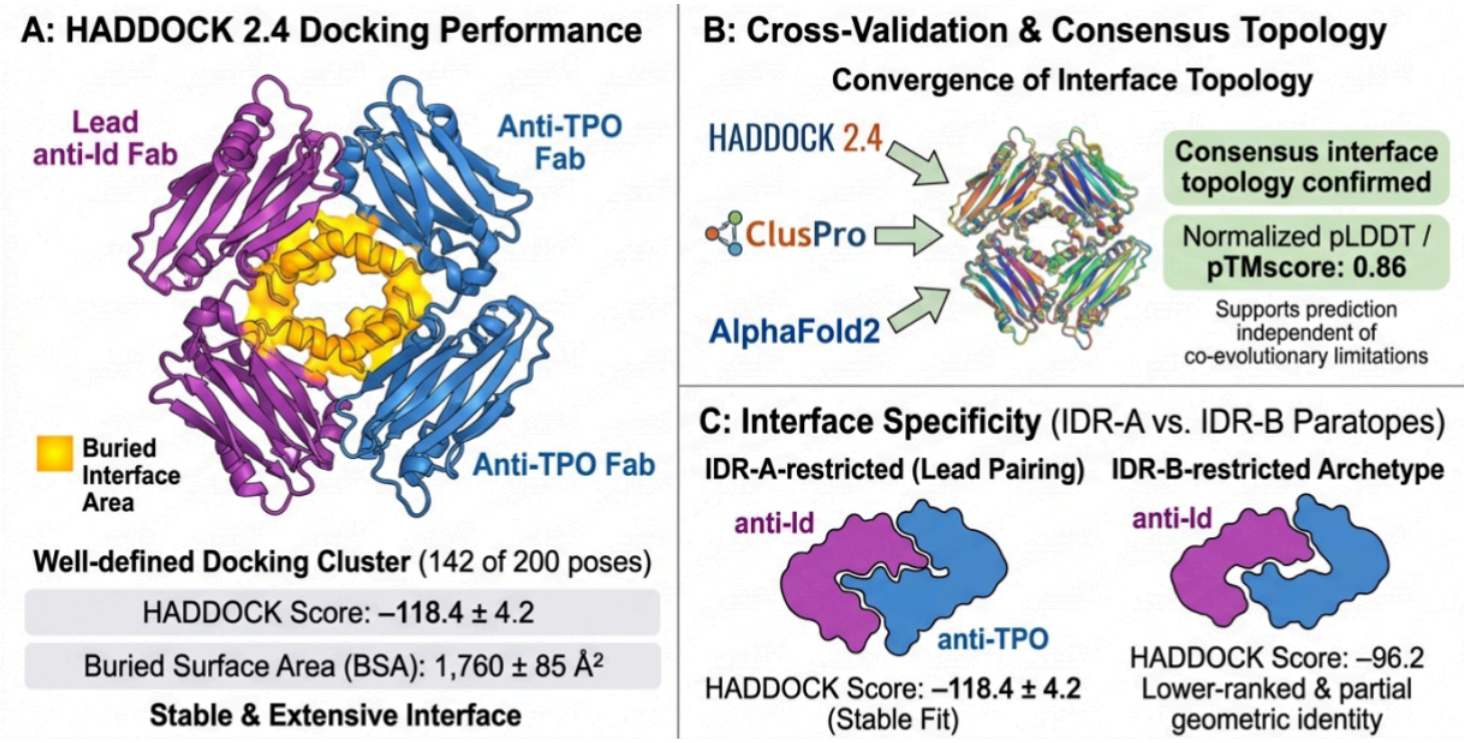


Figure 4

Best-ranked HADDOCK docking pose of the anti-idiotypic Fab in complex with the anti-TPO Fab paratope, with the paratope-paratope interface highlighted and key interacting CDR residues labeled.

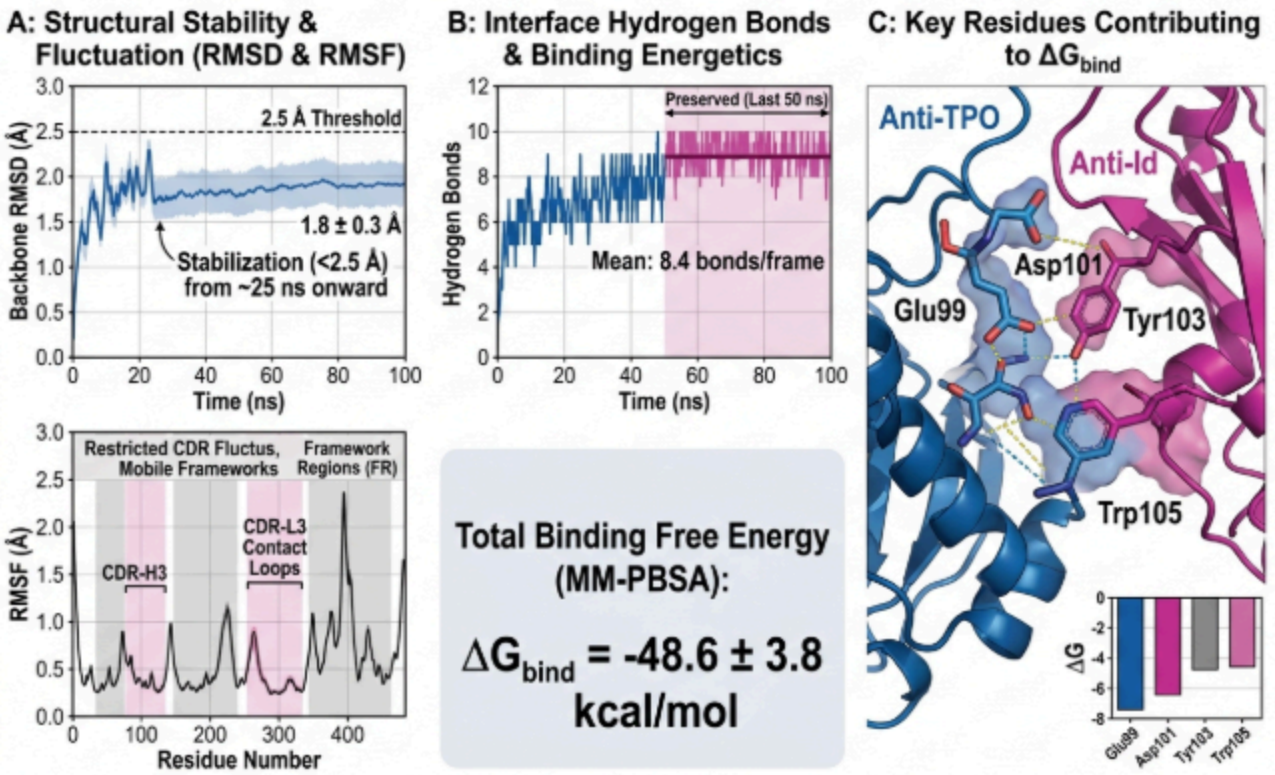


Figure 5

Time evolution of interface RMSD and RMSF for the anti-Id/anti-TPO complex over the 100 ns molecular dynamics trajectory

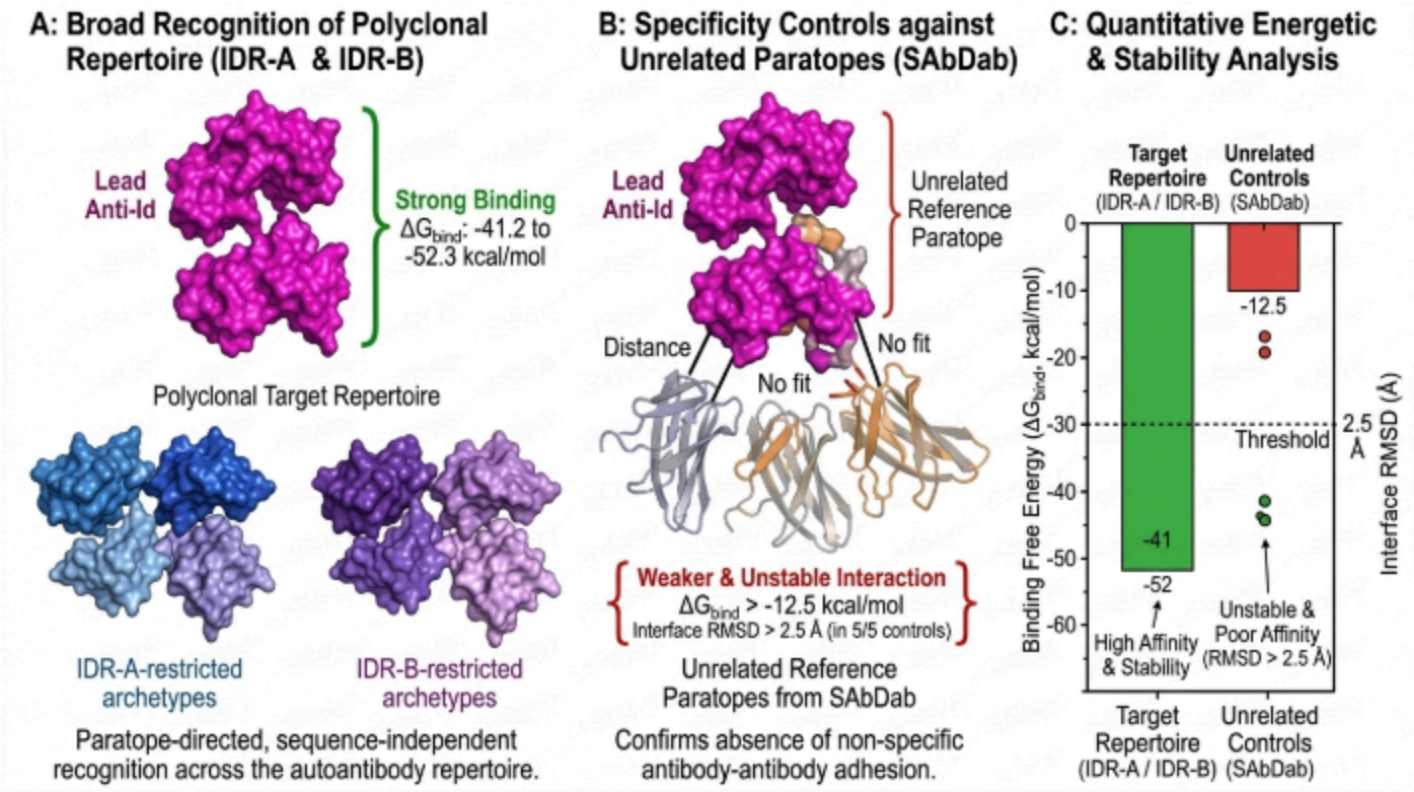


Figure 6

Comparative binding free energy profile of the anti-Id candidate against representative anti-TPO paratope archetypes versus unrelated control paratopes, demonstrating target-restricted specificity